Soft Matter

PAPER

View Article Online
View Journal | View Issue

Cite this: *Soft Matter*, 2016, 12, 9202

Stretchable, adhesive and ultra-conformable elastomer thin films†

Nobutaka Sato,[a] Atsushi Murata,[b] Toshinori Fujie*[cd] and Shinji Takeoka*[a]

Received 31st May 2016,
Accepted 8th October 2016

DOI: 10.1039/c6sm01242f

www.rsc.org/softmatter

Thermoplastic elastomers are attractive materials because of the drastic changes in their physical properties above and below the glass transition temperature (T_g). In this paper, we report that free-standing polystyrene (PS, T_g: 100 °C) and polystyrene–polybutadiene–polystyrene triblock copolymer (SBS, T_g: −70 °C) thin films with a thickness of hundreds of nanometers were prepared by a gravure coating method. Among the mechanical properties of these thin films determined by bulge testing and tensile testing, the SBS thin films exhibited a much lower elastic modulus (*ca.* 0.045 GPa, 212 nm thickness) in comparison with the PS thin films (*ca.* 1.19 GPa, 217 nm thickness). The lower elastic modulus and lower thickness of the SBS thin films resulted in higher conformability and thus higher strength of adhesion to an uneven surface such as an artificial skin model with roughness (R_a = 10.6 μm), even though they both have similar surface energies. By analyzing the mechanical properties of the SBS thin films, the elastic modulus and thickness of the thin films were strongly correlated with their conformability to a rough surface, which thus led to a high adhesive strength. Therefore, the SBS thin films will be useful as coating layers for a variety of materials.

1. Introduction

Elastomers are attractive materials for the biomedical, electronics and coatings fields[1–9] owing to their unique properties including elasticity, flexibility, and toughness. These physical properties are key factors in the choice of materials used in electronic devices,[1,8,9] self-healing materials,[10–12] and wearable devices.[4,13] Elastomers display the characteristic of elongation under external forces instead of breaking up; for instance, chewing gum changes its form to conform to the substrate of teeth. The physical properties of the constituent polymeric chains change from a glassy to a rubbery state at the glass transition temperature (T_g).[14,15] In general, polymers display glassy properties (rigid and fragile) below T_g and rubbery properties (flexible and conformable) above T_g, whereas elastomers exhibit reversible deformation under an external force. Elastomers that have these mechanical properties are generally classified into vulcanized rubbers and thermoplastic elastomers (TPEs). TPEs are composed of soft segments of flexible rubbers and hard segments of rigid resins to prevent plastic deformation.

Ultrathin polymeric films (nanosheets) are expected to be valuable for a wide variety of applications such as in the electrochemical, biomedical, and printing fields.[16–19] Polymeric nanosheets have unique properties including thickness-dependent glass transition temperatures[20,21] and Young's moduli.[22–24] Understanding these physical and mechanical properties of nanosheets enables us to control various functions such as the adhesion and molecular permeability of nanosheets.[25] In particular, the adhesion property of nanosheets is one of the fundamental characteristics for the attachment of nanosheets to various surfaces. Such nanosheets can be attached to silicon wafers and organs including the skin and lungs without chemical glues.[26–28] So far, we have reported the unique mechanical properties of nanosheets that consist of non-elastomeric polyesters[22] and polyelectrolytes[28] by bulge testing and microscratch testing.[29] Interestingly, the adhesive force increases with a reduction in thickness to less than *ca.* 100 nm, which would be due to the high conformability of thinner nanosheets, which would increase the total secondary interaction forces between the nanosheets and an adherend with some roughness. Although these nanosheets exhibited an increase in adhesion depending on their thickness, other factors such as flexibility and surface energy are also largely

[a] *Department of Life Science and Medical Bioscience, Graduate School of Advanced Science and Engineering, Waseda University, TWIns, 2-2 Wakamtsu-cho, Shinjuku-ku, Tokyo 162-8480, Japan. E-mail: takeoka@waseda.jp*
[b] *Institute for Nanoscience and Nanotechnology, Waseda University, 513 Waseda Tsurumaki-cho, Shinjuku, Tokyo 162-0041, Japan*
[c] *Waseda Institute for Advanced Study, Waseda University, TWIns, 2-2 Wakamtsu-cho, Shinjuku-ku, Tokyo 162-8480, Japan. E-mail: t.fujie@aoni.waseda.jp*
[d] *Japan Science and Technology Agency, PRESTO, 4-1-8 Honcho, Kawaguchi, Saitama 332-0012, Japan*

† Electronic supplementary information (ESI) available: Figures and tables showing supplier information for the tape test, mechanical properties of the PS and SBS thin films determined by the bulge test and tensile test, static contact angles of the PS and SBS thin films, and optical properties of the SBS thin film with a thickness of 690 nm using an ultraviolet-visible absorption spectrophotometer. Movies showing stretching of the 212 nm thick SBS thin film, elongation of the 690 nm thick SBS thin film by a tensile tester, and shatterproofness experiments. See DOI: 10.1039/c6sm01242f

associated with adhesion. In particular, flexibility is an important factor that affects adhesive strength on irregularly shaped surfaces. In previous studies, a poly(dimethylsiloxane) (PDMS) nanomembrane displayed high flexibility,[30,31] but the PDMS nanomembrane is not suitable for large-scale fabrication because a thermal curing process that lasts for hours is essential for the PDMS prepolymer. Therefore, we focused our attention on more appropriate elastomers for the fabrication of thin films on a large scale. Elastomeric thin films with a thickness of greater than 100 nm are expected to have both the mechanical properties of a bulk elastomer and the physical properties of conventional non-elastomeric nanosheets with a thickness of *ca.* 100 nm. Understanding the unique physical properties of elastomeric thin films in comparison with those of non-elastomeric thin films is a necessary advance in the nanomaterials field.

In this study, we fabricated highly flexible and stretchable elastomeric thin films and investigated their mechanical and adhesive properties by bulge testing, tensile testing, and cross-cut testing according to ISO 2409 in comparison with a standard polymeric (PS) thin film. These thin films were prepared by a microgravure coating method[18] and were simply detached from a polyethylene terephthalate (PET) substrate by using a water-soluble sacrificial layer of polyvinyl alcohol (PVA). Free-standing thin films were transferred to a silicon wafer or an artificial skin model to characterize their surface morphology, conformability, and adhesive properties. Furthermore, the high adhesion and flexibility of these elastomeric thin films demonstrated mechanical durability by utilizing a shatterproofness experiment.

2. Experimental

Materials

Silicon wafers were purchased from KST World Co. (Fukui, Japan). The silicon wafers were cut into pieces with sizes of 2 cm × 2 cm and immersed in a piranha solution (H_2SO_4/H_2O_2 = 3/1, v/v) at 120 °C for 15 min, followed by being thoroughly rinsed with deionized water (18 MΩ cm) to remove any contaminants adsorbed on the surface. An artificial skin model (Bioskin®, Beaulax Co., Ltd, Saitama, Japan) made from polyurethane was used in SEM observations and a tape test. This artificial skin model has been used in the fields of cosmetics and coating materials.[32–34] It imitates the mechanical properties such as the elastic modulus and roughness of the stratum corneum of human skin, with a tensile strength of 0.95 MPa, an elongation of 480%, and a roughness (R_a) of 10.6 μm. All organic solvents (reagent grade) and poly(vinyl alcohol) (PVA; M_w 22 000, 86.5–89% hydrolyzed) were purchased from Kanto Chemical Co., Inc. (Tokyo, Japan) and were used without purification. Polystyrene-*block*-polybutadiene-*block*-polystyrene (SBS; M_w 140 000) and polystyrene (PS; M_w 280 000) were purchased from Sigma-Aldrich Japan (Tokyo, Japan). The IR and ^{1}H NMR spectra of SBS were recorded and are shown in Fig. S1 (ESI†). The monomer ratio of styrene to butadiene was 1 to 6.8 (butadiene 87 mol%) by calculation from the integral values attributed to styrene and butadiene in the ^{1}H NMR spectrum. The thickness of thin films was determined by AFM (VN-8000, Keyence Co., Ltd, Osaka, Japan).

Preparation of PS and SBS thin films by gravure coating

Both PS and SBS thin films were fabricated by a microgravure technique utilizing a Mini-Labo coater (Yasui Seiki Co., Ltd, Kanagawa, Japan). The thickness of the thin films was controlled *via* the concentration of the polymer solution. A 2 wt% PVA solution was coated on a PET film (12 cm width, Lumirror® L-25T60, Toray Industries Inc., Tokyo, Japan) with a rotation speed of the gravure roll of 30 rpm, a line speed of 1.3 m min^{-1} and a drying temperature of 100 °C. SBS and PS were dissolved in tetrahydrofuran (THF) and ethyl acetate, respectively. After filtration with a syringe filter (SupraPure®, 0.2 μm, Recenttec Inc.), these polymer solutions were coated on PVA/PET films under the same conditions used for coating with PVA, except for the use of a drying temperature of 80 °C. The resulting polymeric thin film was released from the PET substrate by immersion in water to dissolve the sacrificial PVA layer. In measuring the thickness of PS and SBS thin films, firstly, both edges of a PS or SBS film coated on PET (1 m in length and 12 cm in width) were trimmed by about 1 cm. Next, three areas of this film were randomly selected, cut into pieces, and then transferred to silicon wafers. The average thickness and standard deviation of each polymeric thin film were calculated from measurements of three locations on each piece by AFM.

AFM observations of thin films on a silicon wafer

Atomic force microscopy (AFM, Innova SPM, Bruker Co., Ltd, MA, USA) was used to investigate the surface morphologies and to perform analyses of the surface of PS and SBS thin films on silicon wafers. AFM measurements were carried out with a piezo scanner (maximum scan size of 50 μm × 50 μm) at room temperature. Commercially available cantilever-style tapping mode tips (RTESPA-CP silicon AFM probes, Bruker Co., Ltd) were used with a resonance frequency in the range of 290–330 kHz. AFM tapping phase images were filtered and analyzed by NanoScope Analysis software (Bruker).

SEM observations of thin films on an artificial skin model

The surface morphologies of the PS and SBS thin films on an artificial skin model (R_a = 10.6 ± 1.8 μm) were investigated by SEM (VE-9800, Keyence Co., Ltd, Osaka, Japan). The thin films were transferred onto the artificial skin model from a free-standing state at an air–water interface using a mesh.

Measurement of contact angle

Free-standing PS and SBS thin films were transferred onto a silicon wafer and dried *in vacuo*. Then, 4 μL Milli-Q water was dropped onto the thin film and the contact angle was measured within 30 s after deposition of the droplet. Young's eqn (1) describes the principle of the contact angle:[35]

$$\gamma_s = \gamma_{sl} + \gamma_l \cos\theta \quad (1)$$

where θ, γ_s, γ_l, and γ_{sl} represent the contact angle, free energy of the solid surface, free energy of the liquid surface, and solid–liquid interfacial energy, respectively.

The work of adhesion between a solid surface and a liquid can be represented by eqn (2) and (3):[36,37]

$$W_{sl} = \gamma_s + \gamma_l - \gamma_{sl} \quad (2)$$

Eqn (1) and (2) are combined, resulting in eqn (3)

$$W_{sl} = \gamma_l(1 + \cos\theta) \quad (3)$$

Analysis of mechanical properties of thin films by a bulge test

A bulge test was performed as described in previous studies.[38–40] In order to determine the ultimate tensile strength and elastic modulus of the thin films, the following equations were used:

$$\sigma = \frac{P \times a^2}{4 \times h \times d} \quad (4)$$

$$\varepsilon = \frac{2 \times d^2}{3 \times a^2} \quad (5)$$

$$E = \frac{\sigma}{\varepsilon} \quad (6)$$

where σ, P, a, h, d, ε and E represent the tensile stress, applied pressure, radius of the circular hole in the steel plate, thickness, deflection, tensile strain, and elastic modulus of the thin film, respectively.

Analysis of mechanical properties of thin films by a tensile test

A tensile test of the PS and SBS thin films was performed at 23 ± 2 °C and a humidity of 50 ± 5% using a tensile tester (EZ-S-5N, Shimadzu Co., Ltd, Kyoto, Japan) with a tensile speed of 10 mm min^{-1} according to ISO 3270. Mechanical data such as normal stress and normal strain were calculated by TRAPEZIUM X analysis software (Shimadzu). From the stress–strain curves, the tensile strength, elongation and Young's modulus (strain 2.5–5%) of the thin films were calculated.

Shatterproofness experiment

PS and SBS thin films with thicknesses of 697 nm and 690 nm were attached to cover glasses (22 mm × 22 mm, thickness 0.12–0.17 mm, Matsunami Glass Co., Ltd, Osaka, Japan), respectively. Prior to the shatterproofness experiment, the glass substrates were kept in an environmental chamber for 24 h (temperature 23 °C, humidity 50%). Then, the substrates were smashed by a household hammer (head weight: 57 g).

Measurement of adhesive strength of thin films on an artificial skin model by a tape test

The adhesive strength of the PS and SBS thin films on an artificial skin model was determined by a tape test according to ISO 2409. The temperature and humidity were controlled *via* an environmental chamber (KCL-2000A, Tokyo Rikakikai Co., Ltd, Tokyo, Japan) at 32 ± 2 °C and 50 ± 5% in accordance with ISO 3270. The thin films were transferred onto the artificial skin model from a free-standing state at an air–water interface using a mesh. The thin films were peeled off from the artificial skin model using standard tape (Cellophane tape CT-24, Nichiban Co., Ltd, Tokyo, Japan) with an adhesive strength of 4.0 N cm^{-1} and other tapes having different adhesive strengths from 0.08 to 4.0 N cm^{-1} (Table S1, ESI†). The data were classified by a number from 0 to 5, depending on the size of the detached area. Detached areas of greater than 65%, 35–65%, 15–35%, 5–15%, less than 5%, and 0% were classified as 5, 4, 3, 2, 1, and 0, respectively. The adhesive strength of each tape was determined according to ISO 29862–29864.

3. Results and discussion

PS and SBS thin films were fabricated by a microgravure coating method on a PVA-coated PET film. After gradually detaching the thin films from the PET substrate by dissolving the PVA layer in water, the resulting free-standing thin film floating at an air–water interface, as shown in Fig. 1a, could be easily scooped onto a silicon wafer for measurements of thickness. The SBS thin film with a thickness of 690 nm was stretchable, as shown in Fig. 1b. The PS thin films fabricated from 2, 2.5, and 7 wt% solutions in ethyl acetate had thicknesses of 127 ± 10 nm, 217 ± 5 nm and 697 ± 7 nm, respectively, whereas the thicknesses of SBS thin films fabricated from 1, 2, 2.5, and 4 wt% solutions in tetrahydrofuran (THF) are shown in Fig. 1c. As predicted from the data for the PS thin films, the thickness of the SBS thin films

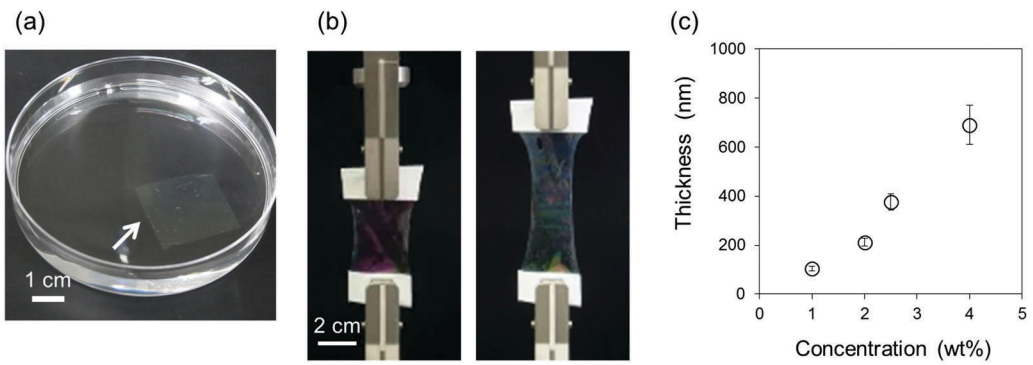

Fig. 1 Membrane stability on water and control of thickness of SBS thin films. (a) Free-standing 212 nm-thick SBS thin film (shown by white arrow, 2 cm × 2 cm) at an air–water interface. (b) Free-standing 690 nm-thick SBS thin film stretched by a tensile tester. (c) Relationship between the concentration of the solution of SBS in THF and the thickness of the resulting SBS thin films.

Table 1 Mechanical properties of PS and SBS thin films with different thicknesses determined by a bulge test

Polymer	Thickness (nm)	Ultimate tensile strength (MPa)	Ultimate tensile elongation (%)	Elastic modulus (GPa)
PS	127 ± 10	16 ± 3	6.3 ± 2.4	0.90 ± 0.05
PS	217 ± 5	16 ± 3	4.4 ± 1.1	1.19 ± 0.33
SBS	212 ± 16	1.4 ± 0.2	18.2 ± 5.1	0.045 ± 0.025
SBS	690 ± 79	1.2 ± 0.3	19.8 ± 14.4	0.059 ± 0.026

depended on the concentration of the SBS solution. The average thicknesses were used for a bulge test and a tensile test.

As shown in Tables 1 and 2, we prepared five samples and investigated them: PS thin films with thicknesses of 127 nm (conventional nanosheet), 217 nm, and 697 nm were used as standard samples, and SBS thin films with similar thicknesses to those of the two thicker PS films, one with a thickness of 212 nm (thinner SBS thin film) and one with a thickness of 690 nm (thicker SBS thin film) were compared with the three PS thin films. Movie S1 (shown in ESI†) demonstrates the stretchable nature of the 212 nm SBS film: it could be stretched with tweezers from 1 cm to *ca.* 3 cm and returned to its original size after being released from the tweezers. However, the 217 nm PS film could not be stretched but fractured under the same treatment. Thus, the PS thin film was not able to sustain a self-supporting state in air.

Next, the surface morphology and wettability of the PS and SBS thin films were observed, as shown in Fig. 2 and Fig. S2 (ESI†). Firstly, the surface morphologies of the 217 and 697 nm PS films and the 212 and 690 nm SBS films on silicon wafers were observed by atomic force microscopy (Fig. 2a–d). The 212 and 690 nm SBS films were stretched (100% tensile elongation) by a tensile tester and were then transferred onto silicon wafers (Fig. 2e and f). The surface of the 217 nm PS film was flat (Fig. 2a), whereas that of the 697 nm PS film was phase-separated owing to supersaturation and the average diameter of polystyrene domains was about 150 nm (Fig. 2b). On the other hand, the SBS thin films were phase-separated into polystyrene and polybutadiene domains (Fig. 2c and d). In previous studies,[41–43] the surfaces of an SBS thin film adopted various phase-separated structures consisting of polystyrene cylinders and/or spheres in a polybutadiene matrix. According to tapping phase images and the abovementioned previous studies, the bright domains and dark domains are attributed to polystyrene and polybutadiene, respectively. The polystyrene domains in the 212 nm SBS film were larger than those in the 690 nm film. Therefore, polystyrene domains would easily aggregate when the thinner SBS films were fabricated in a polymer solution (20 mg mL^{-1}) with a lower viscosity. The thickness of the films depended on the concentration of the polymer solutions: the thin films were fabricated from low-concentration polymer solutions. Furthermore, orientation of styrene domains was observed on the surface of elongated SBS thin films with thicknesses of 212 nm and 690 nm (Fig. 2e and f).

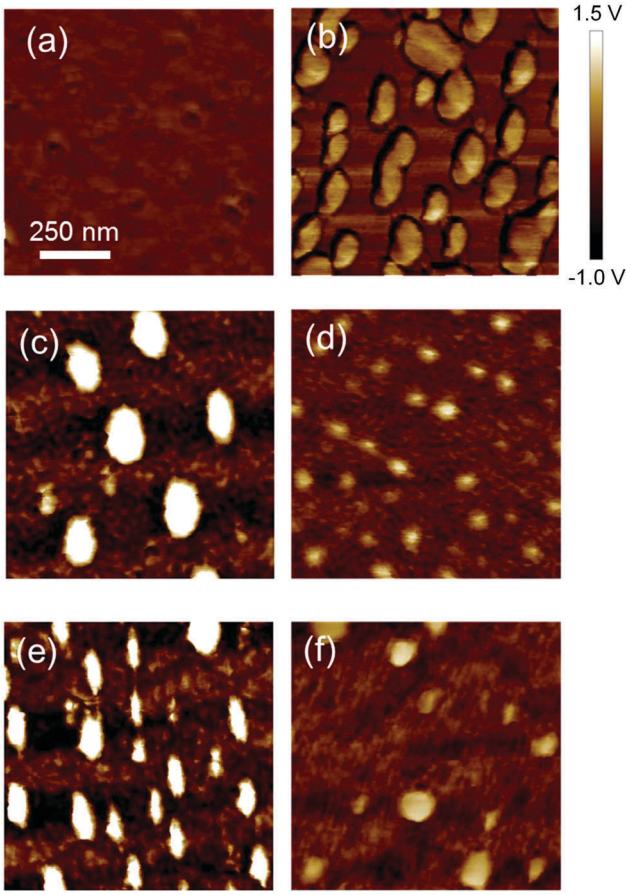

Fig. 2 (a)–(d) AFM images of PS thin films with thicknesses of 217 nm (a) and 697 nm (b), SBS thin films with thicknesses of 212 nm (c) and 690 nm (d), and SBS thin films with thicknesses of 212 nm (e) and 690 nm (f), which were elongated (the elongation ratio was 100%) using a tensile tester.

Table 2 Adhesive strength scores of thin films on an artificial skin model determined by a cross-cut tape test. Detached areas of greater than 65%, 35–65%, 15–35%, 5–15%, less than 5%, and 0% were scored as 5, 4, 3, 2, 1, and 0, respectively

Adhesive strength (N cm^{-1})	PS 127 nm	PS 217 nm	PS 697 nm	SBS 212 nm	SBS 690 nm
4.01	5	5	5	5	5
2.59	—	—	—	5	—
1.18	—	—	—	5	—
1.06	—	—	—	5	—
0.78	—	—	—	0	5
0.71	—	—	—	—	5
0.29	5	—	—	—	0
0.22	5	—	—	0	0
0.18	5	—	—	—	—
0.08	1	5	5	—	—

The wettability of the thin films was determined by measurements of the contact angle using a droplet of Milli-Q water (Fig. S2, ESI†). The static contact angles of the 127 nm, 217 nm, and 697 nm PS films and the 212 and 690 nm SBS films were 77 ± 2°, 76 ± 1°, 78 ± 2°, 82 ± 1°, and 83 ± 1°, respectively. In addition, the static contact angle of an artificial skin model was 114 ± 3°. The adhesion energies of the thin films are shown in Table S3 in the ESI.† In general, although wettability is a critical factor for adhesion, this table indicated that the wettabilities of

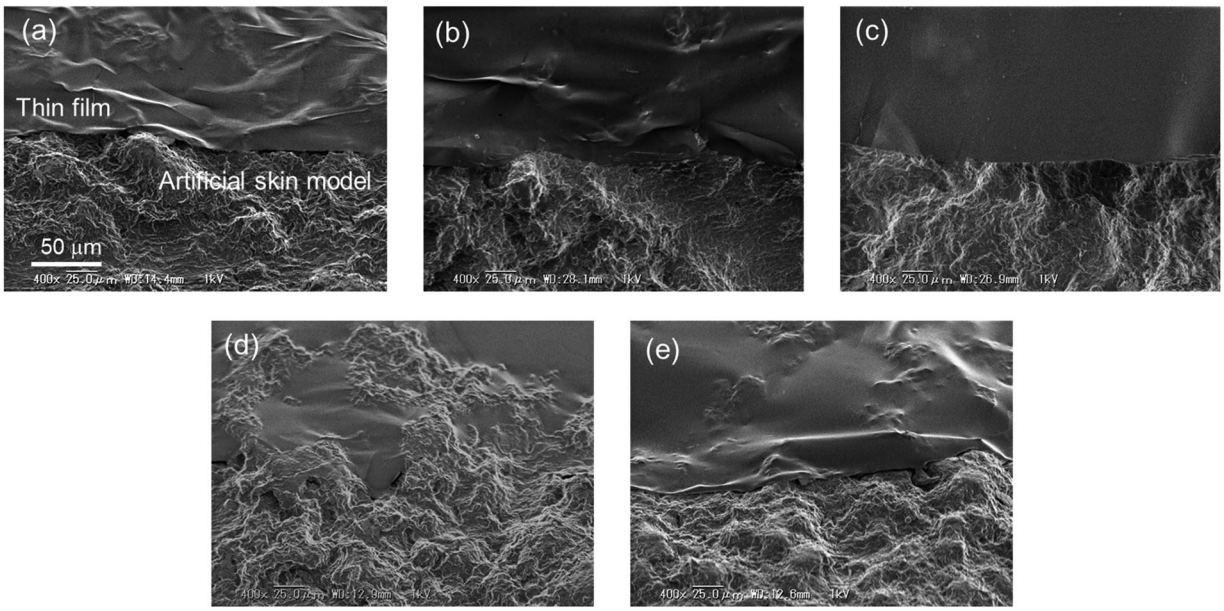

Fig. 3 SEM images at the edges of the PS (a)–(c) and SBS (d) and (e) thin films on an artificial skin model (R_a = 10.6 μm). The thicknesses of these thin films were (a) 127 nm, (b) 217 nm, (c) 697 nm, (d) 212 nm, and (e) 690 nm.

the PS and SBS thin films were much the same. Therefore, wettability would not be a factor in the strength of adhesion of the thin films to an artificial skin model. The conformability of the PS and SBS thin films to an artificial skin model was examined by SEM (Fig. 3).

SEM images of the 127, 217, and 697 nm PS films and the 212 and 690 nm SBS films on the artificial skin model are shown in Fig. 3a–e, respectively. The thinnest PS film (127 nm) exhibited the highest conformability to the rough surface (Fig. 3a–c). In addition, the thinner SBS film (212 nm, Fig. 3d) was more conformable than the thicker film (690 nm, Fig. 3e). Thus, it is indicated that conformability to the rough surface depended on the thickness of the thin films. Furthermore, the 217 nm PS film did not conform to the rough surface (Fig. 3b), whereas the 212 nm SBS film clearly conformed to the rough surface and the boundary between the SBS thin film and the artificial skin model was obscure (Fig. 3d). Similarly, the thicker 690 nm SBS film was much more conformable than the similarly thick 697 nm PS thin film. These results indicated that the shape-matching ability of the thin films was dependent on their thickness and the type of polymer: in this case, the presence of a rich butadiene content (87 mol% butadiene units) in the polymeric chain. Some mechanical properties of the thin films were studied by a bulge test. Cross-sectional views of the deflection of four thin film samples at pressures of 0.2–0.8 kPa are shown in Fig. S3 in the ESI,† and those at a pressure of 0.8 kPa are representatively shown in Fig. 4a. The 212 nm SBS film was highly deflected in comparison to the 217 nm PS film, which had a similar thickness. It displayed a larger deflection than that of the 690 nm SBS film, and even the 690 nm SBS film displayed a larger deflection than that of the thinnest PS film (127 nm). The ultimate tensile strength and elastic modulus of each thin film were calculated as described in the experimental section (eqn (4)–(6)). Pressure-deflection curves of the four PS and SBS thin films are shown in Fig. 4b. The slopes of the curves indicated that the SBS films were deflected in regions of lower pressure in comparison with the PS films, and the thinner SBS film exhibited a higher rate of deflection at the same pressure than the thicker film. These pressure-deflection curves were converted into stress–strain curves (Fig. 4c), and the ultimate tensile strength, ultimate tensile elongation, and elastic modulus were calculated from the initial elasticity of the stress–strain curve for each thin film and are listed in Table 1. The elastic moduli of the thinner and thicker SBS films were 0.045 ± 0.025 GPa and 0.059 ± 0.026 GPa, respectively. Thus, the thinner and thicker SBS films had similar elastic moduli in each case.

Owing to the presence of the butadiene part of the polymer chain, the 212 nm SBS film exhibited an ultimate tensile strength that was *ca.* 11 times lower, an ultimate tensile elongation that was *ca.* 4 times greater, and an elastic modulus that was *ca.* 26 times lower in comparison with those of the 217 nm PS film. In a previous study of an elastomeric thin film,[39] polyurethane (PU) thin films were fabricated by cross-linking acryl urethane resin. The PU thin film exhibited an elongation of 33.6% and a tensile strength of 10 MPa. On the other hand, the SBS thin film exhibited an elongation of 19% and a tensile strength of 1.3 MPa, respectively. As these elastomers consisted of soft and hard segments, the employment of elastomers for the fabrication of thin films enabled the softening of the thin films so that their tensile strength was in the MPa range (*i.e.*, the soft and hard segments of PU are attributed to the alkyl chains of the polyol and urethane domains, whereas those of SBS are attributed to the butadiene and styrene domains). In addition, in our previous studies[27,28] poly(L-lactic acid) (PLLA) thin films and polysaccharide thin films composed of chitosan and sodium alginate were fabricated. The elastic moduli of a

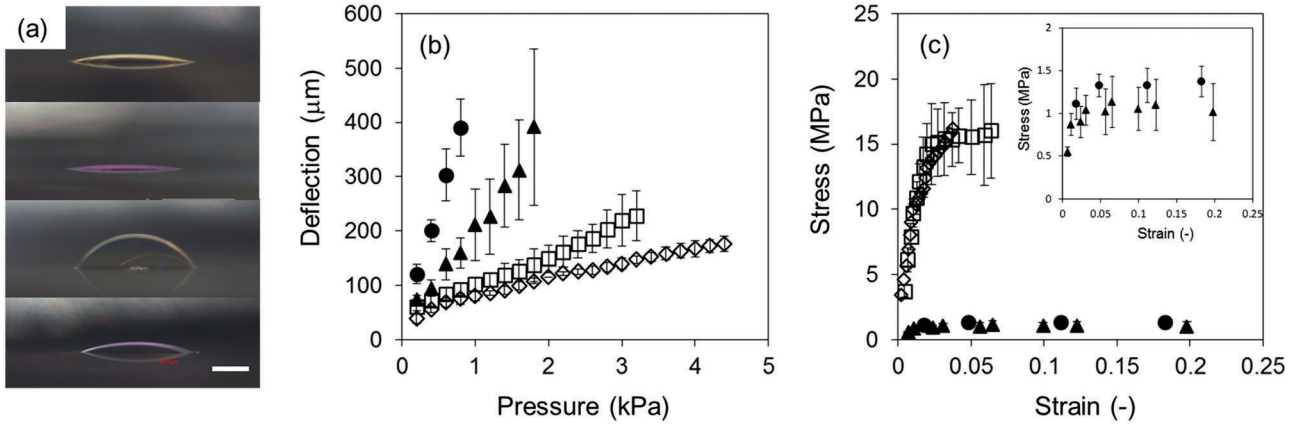

Fig. 4 Determination of mechanical properties of the thin films. (a) Sequential cross-sectional views of the deflections at a pressure of 0.8 kPa of the PS thin films with thicknesses of 127 nm and 217 nm and SBS thin films with thicknesses of 212 nm and 690 nm, in order from the top. n = 3. Scale bar: 500 μm. (b) Pressure-deflection and (c) stress–strain curves of the PS thin films with thicknesses of 127 nm (□) and 217 nm (◇) and SBS thin films with thicknesses of 212 nm (●) and 690 nm (▲). The inset shows a magnified plot for the SBS thin films.

23 nm PLLA film and a 35 nm polysaccharide film were 1.7 GPa and 1.1 GPa, respectively. Thus, the elastic moduli of the SBS thin films were much lower than those of the other thin films in spite of the fact that their thicknesses were greater than 200 nm. Furthermore, considering the fact that the elastic moduli of the other films were in the GPa range, employing elastomers could contribute to a reduction in the elastic modulus from the GPa range to the MPa range.

In addition to the bulge test, the mechanical properties of the 212 and 690 nm SBS films and the 697 nm PS film were investigated using a tensile tester. The behavior of the 690 nm SBS film under loading by the tensile tester is representatively shown in Movie S2 in the ESI.† The tensile strength, elongation, and Young's modulus of these thin films were calculated from the stress–strain curves determined from the tensile test (Fig. S4 and Table S2, ESI†). The tensile strength of the 697 nm PS film was 5.4 MPa, which was *ca.* 6 times higher than those of the thicker and thinner SBS films. In general, the tensile strengths of bulk PS and SBS are 45–60 MPa[44] and 2.5–30 MPa,[45] respectively. In comparison with those of the bulk polymers, the values of 5.4 MPa for the PS thin film and *ca.* 1 MPa for the SBS thin film were quite low. The elongation of the 697 nm PS film was 1.8%, which was *ca.* 100 times less than that of the 690 nm SBS film. The Young's modulus of the 697 nm PS film was 0.52 GPa, whereas those of the 212 and 690 nm SBS films were 5.7 ± 1.2 MPa and 4.9 ± 0.8 MPa, respectively. Thus, the SBS thin film exhibited a thickness-independent Young's modulus and a much lower Young's modulus in comparison with that of the PS thin film with a similar thickness. These results indicated that the mechanical properties such as the elastic modulus and Young's modulus strongly depended on the types of polymers used rather than the thickness of the thin film.

In addition, SEM observations (Fig. 3) demonstrated that the elastomeric SBS thin films expanded and contracted at very low stresses and conformed to a substrate with a rough surface, because the elastic modulus of the SBS thin film was *ca.* 26 times less than that of the PS thin film.

Next, the adhesive strengths of the thin films were determined according to the cross-cut test described in ISO 2409 with scoring from 0 to 5 under strict control of the temperature (32 °C) and humidity (50%) using an environmental control chamber and a glove box. At first, an artificial skin model and Cellophane® tape were used as an adherend and a pressure-sensitive adhesive tape, respectively. All thin films were easily detached from the artificial skin model when Cellophane® tape with an adhesive strength of 4.01 N cm^{-1} was used. Therefore, various tapes with different adhesive strengths of less than 4.01 N cm^{-1} were used for the cross-cut test, and the results are summarized in Table 2. The adhesive strengths of the 127 nm PS film and the 212 and 690 nm SBS films were estimated to be 0.08–0.18 N cm^{-1}, 0.78–1.06 N cm^{-1}, and 0.29–0.71 N cm^{-1}, respectively. Also, the adhesive strengths of the 217 and 697 nm PS films were estimated to be less than 0.08 N cm^{-1}. In general, the 212 nm SBS film displayed the strongest adhesion and even the 690 nm SBS film had a much greater adhesive strength than that of the thinnest PS film (127 nm). Therefore, it is suggested that the strength of adhesion to the artificial skin model was influenced by the conformability of the thin films, which was related to the elastic modulus and thickness of the thin films.

Finally, the SBS thin films exhibited mechanical durability, as was shown by conducting a shatterproofness experiment. The 697 nm PS and 690 nm SBS films were attached to cover glasses (22 mm × 22 mm, thickness 0.12–0.17 mm) and kept in an experimental chamber (temperature 23 °C, humidity 50%) for 24 h. Then, a pristine cover glass and the samples were smashed by a hammer (Movie S3, ESI†). In general, rubbers and elastomers such as TPE and silicone resin are used for shatter-proof materials for window glass and liquid crystal displays owing to their high elasticity for shock absorption. The pristine cover glass and that with an attached PS thin film were scattered in all directions (Movie S3a and b, ESI†), whereas the cover glass with an attached SBS thin film was not scattered; the smashed glass was supported by the SBS thin film and could

then be picked up with tweezers (Movie S3c, ESI†). The adhesion of the SBS thin film to the glass was sufficiently strong in spite of its submicron thickness. The low elastic modulus of the SBS thin film was probably responsible for the fact that it prevented the cover glass from being scattered. These results suggest that the SBS thin film could be used for coating materials. The transmittance of the 690 nm SBS film was approximately 100% in the wavelength region from 300 to 800 nm because of its submicron thickness (Fig. S5, ESI†). Taken together, these results suggest that the SBS thin films are good candidates for employment as coating materials to protect electronic devices.

4. Conclusions

We fabricated free-standing elastomeric thin films made from SBS using a microgravure coating method. The mechanical and adhesive properties of the elastomeric SBS and standard polymeric PS thin films were compared in this study. The SBS thin films displayed a much lower elastic modulus and a higher adhesive strength in comparison with those of PS films with a similar thickness owing to the presence of the butadiene part of the polymer chain. Although the elastic modulus of the SBS thin films did not depend on their thickness, the thinner SBS film was more conformable and had a greater adhesive strength than the thicker SBS film. Therefore, the elastic modulus and thickness appear to be correlated with the conformability to a rough surface, which then determines the adhesive strength. These results indicate that the adhesive strength is controllable *via* the elastic modulus and thickness rather than the free energy, as both SBS and PS have similar free energies. The SBS thin films had high mechanical stability, adhered to rough surfaces, and have a high probability of acting as excellent coating materials.

Acknowledgements

This work was partially supported by JSPS KAKENHI: Grant Number 25289252 (S. T.), 15H05355 (T. F.) from MEXT, Japan, the Precursory Research for Embryonic Science and Technology (PRESTO): Grant Number 15655478 (T. F.) from the Japan Science and Technology Agency, and Mizuho Foundation for the Promotion of Sciences (T. F.).

Notes and references

1 D.-H. Kim, J.-H. Ahn, W. M. Choi, H. Kim, T. Kim, J. Song, Y. Y. Huang, Z. Liu, C. Lu and J. A. Rogers, *Science*, 2008, **320**, 507–511.
2 S.-I. Park, Y. Xiong, R.-H. Kim, P. Elvikis, M. Meitl, D.-H. Kim, J. Wu, J. Yoon, C.-J. Yu, Z. Liu, Y. Huang, K.-C. Hwang, P. Ferreira, X. Li, K. Choquette and J. A. Rogers, *Science*, 2009, **325**, 977–981.
3 Y. Wang, G. A. Ameer, B. J. Sheppard and R. Langer, *Nat. Biotechnol.*, 2002, **20**, 602–606.
4 G. S. Jeong, D.-H. Baek, H. C. Jung, J. H. Song, J. H. Moon, S. W. Hong, I. Y. Kim and S.-H. Lee, *Nat. Commun.*, 2012, **3**, 977.
5 C. L. E. Nijst, J. P. Bruggeman, J. M. Karp, L. Ferreira, A. Zumbuehl, C. J. Bettinger and R. Langer, *Biomacromolecules*, 2007, **8**, 3067–3073.
6 G. C. Engelmayr Jr, M. Cheng, C. J. Bettinger, J. T. Borenstein, R. Langer and L. E. Freed, *Nat. Mater.*, 2008, **7**, 1003–1010.
7 B. Yu, S.-Y. Kang, A. Akthakul, N. Ramadurai, M. Pilkenton, A. Patel, A. Nashat, D. G. Anderson, F. H. Sakamoto, B. A. Gilchrest, R. R. Anderson and R. Langer, *Nat. Mater.*, 2016, **15**, 911–918.
8 J. Liang, L. Li, X. Niu, Z. Yu and Q. Pei, *Nat. Photonics*, 2013, **7**, 817–824.
9 C. Larson, B. Peele, S. Li, S. Robinson, M. Totaro, L. Beccai, B. Mazzolai and R. Shepherd, *Science*, 2016, **351**, 1071–1074.
10 L. Zhu and R. P. Wool, *Polymer*, 2006, **47**, 8106–8115.
11 D. A. Davis, A. Hamilton, J. Yang, L. D. Cremar, D. V. Gough, S. L. Potisek, M. T. Ong, P. V. Braun, T. J. Martínez, S. R. White, J. S. Moore and N. R. Sottos, *Nature*, 2009, **459**, 68–72.
12 Y. Chen, A. M. Kushner, G. A. Williams and Z. Guan, *Nat. Chem.*, 2012, **4**, 467–472.
13 S. Bauer, *Nat. Mater.*, 2013, **12**, 871–872.
14 J. A. Forrest and K. Dalnoki-Veress, *J. Polym. Sci., Part B: Polym. Phys.*, 2001, **39**, 2664–2670.
15 J. Perez and J. Y. Cavaillé, *J. Non-Cryst. Solids*, 1994, **172-174**, 1028–1036.
16 W. Cheng, M. J. Campolongo, S. J. Tan and D. Luo, *Nano Today*, 2009, **4**, 482–493.
17 R. R. Costa and J. F. Mano, *Chem. Soc. Rev.*, 2014, **43**, 3453–3479.
18 R. R. Sondergaard, M. Hosel and F. C. Krebs, *J. Polym. Sci., Part B: Polym. Phys.*, 2013, **51**, 16–34.
19 K. Ariga, Y. Yamauchi, G. Rydzek, Q. Ji, Y. Yonamine, K. C.-W. Wu and J. P. Hill, *Chem. Lett.*, 2014, **43**, 36–68.
20 J. L. Keddie, R. A. L. Jones and R. A. Cory, *Europhys. Lett.*, 1994, **27**, 59–64.
21 N. Satomi, A. Takahara and T. Kajiyama, *Macromolecules*, 1999, **32**, 4474–4476.
22 T. Fujie, L. Ricotti, A. Desii, A. Menciassi, P. Dario and V. Mattoli, *Langmuir*, 2011, **27**, 13173–13182.
23 C. M. Stafford, C. Harrison, K. L. Beers, A. Karim, E. J. Amis, M. R. Vanlandingham, H.-C. Kim, W. Volksen, R. D. Miller and E. E. Simonyi, *Nat. Mater.*, 2004, **3**, 545–550.
24 A. J. Nolte, R. E. Cohen and M. F. Rubner, *Macromolecules*, 2006, **39**, 4841–4847.
25 T. Fujie, Y. Kawamoto, H. Haniuda, A. Saito, K. Kabata, Y. Honda, E. Ohmori, T. Asahi and S. Takeoka, *Macromolecules*, 2013, **46**, 395–402.
26 T. Fujie, Y. Okamura and S. Takeoka, *Adv. Mater.*, 2007, **19**, 3549–3553.
27 Y. Okamura, K. Kabata, M. Kinoshita, D. Saitoh and S. Takeoka, *Adv. Mater.*, 2009, **21**, 4388–4392.
28 T. Fujie, N. Matsutani, M. Kinoshita, Y. Okamura, A. Saito and S. Takeoka, *Adv. Funct. Mater.*, 2009, **19**, 2560–2568.
29 N. Kyouno, D. Arai, K. Takeshita and S. Baba, *J. Adhes. Sci. Technol.*, 2009, **23**, 1973–1991.
30 E. Kang, J. Ryoo, G. S. Jeong, Y. Y. Choi, S. M. Jeong, J. Ju, S. Chung, S. Takayama and S.-H. Lee, *Adv. Mater.*, 2013, **25**, 2167–2173.

31 A. L. Thangawng, R. S. Ruoff, M. A. Swartz and M. R. Glucksberg, *Biomed. Microdevices*, 2007, **9**, 587–595.
32 N. Kitamura, J. Chim and N. Miki, *J. Micromech. Microeng.*, 2015, **25**(2), 025016.
33 Y. Nishinaka, R. Jun, G. S. Prihandana and N. Miki, *Jpn. J. Appl. Phys.*, 2013, **52**(6S), 06GL10.
34 N. Ikeda, K. Miyashita, R. Hikima and S. Tominaga, *Color Res. Appl.*, 2014, **39**, 45–55.
35 T. Young, *Trans. R. Soc.*, 1805, **95**, 65–87.
36 S. Zhandarov and E. Mäder, *Compos. Interfaces*, 2003, **10**, 41–59.
37 B. Bouali, F. Ganachaud, J.-P. Chapel, C. Pichot and P. Lanteri, *J. Colloid Interface Sci.*, 1998, **208**, 81–89.
38 S. Markutsya, C. Jiang, Y. Pikus and V. V. Tsukruk, *Adv. Funct. Mater.*, 2005, **15**, 771–780.
39 H. Watanabe, T. Ohzono and T. Kunitake, *Macromolecules*, 2007, **40**, 1369–1371.
40 T. Fujie, S. Furutate, D. Niwa and S. Takeoka, *Soft Matter*, 2010, **6**, 4672–4676.
41 C. Park, J. Yoon and E. L. Thomas, *Polymer*, 2003, **44**, 6725–6760.
42 L. Peponi, A. Tercjak, J. Gutierrez, H. Stadler, L. Torre, J. M. Kenny and I. Mondragon, *Macromol. Mater. Eng.*, 2008, **293**, 568–573.
43 Q. Zhang, O. K. C. Tsui, B. Du, F. Zhang, T. Tang and T. He, *Macromolecules*, 2000, **33**, 9561–9567.
44 Kagaku Binran Ouyokagakuhen, The Chemical Society of Japan Ed., Maruzen, Tokyo, 7th edn, 2014, p. II-1137.
45 Kagaku Binran Kisohen, The Chemical Society of Japan Ed., Maruzen, Tokyo, 5th edn, 2004, p. I-721.